

**Coulomb breakup in a transformed harmonic oscillator basis**A. M. Moro,<sup>1</sup> F. Pérez-Bernal,<sup>2</sup> J. M. Arias,<sup>1</sup> and J. Gómez-Camacho<sup>1</sup><sup>1</sup>*Departamento de Física Atómica, Molecular y Nuclear, Facultad de Física, Universidad de Sevilla, Apartado 1065, E-41080 Sevilla, Spain*<sup>2</sup>*Departamento de Física Aplicada, Universidad de Huelva, E-21071 Huelva, Spain*

(Received 31 January 2006; published 28 April 2006)

The problem of Coulomb breakup in the scattering of a two-body loosely bound projectile by a heavy target is addressed. A basis of transformed harmonic oscillator (THO) wave functions is used to discretize the projectile continuum and to diagonalize the Hamiltonian of the two-body system. Results for the reaction  ${}^8\text{B}+{}^{58}\text{Ni}$  at sub-Coulomb energies are presented. Comparison of different observables with those obtained with the standard continuum discretized coupled-channels (CDCC) method shows good agreement between both approaches.

DOI: [10.1103/PhysRevC.73.044612](https://doi.org/10.1103/PhysRevC.73.044612)

PACS number(s): 24.10.-i, 25.60.Gc, 25.70.Mn, 25.10.+s

**I. INTRODUCTION**

The collision of a weakly bound system with a target represents a challenging and interesting problem in quantum physics, including atomic, molecular and nuclear physics. A proper understanding of the process requires an appropriate treatment of the unbound part of the spectrum of the loosely bound system. In nuclear collisions, the problem was first addressed in the context of deuteron scattering. One of the first successful approaches to this problem was the continuum discretized coupled-channels (CDCC) method, firstly introduced by Rawitscher [1], and later developed and employed by other groups [2–4]. Within the CDCC method, the reaction process of a loosely two-body projectile and a heavy structureless target is treated within a three-body picture. The idea of the method is to represent the continuum part of the two-body projectile spectrum by a finite set of square integrable states. To this end, the continuum is divided into a finite set of energy intervals. For each interval, or bin, a representative function is constructed by superposition of true scattering wave functions within that interval. By construction, the set of functions obtained in this way are normalizable and mutually orthogonal. By projecting the Schrödinger equation onto the bound and bin wave functions, a set of coupled equations is obtained. The method has been extremely successful and is a reliable reference for any other alternative method. In spite of this, it has been criticized by some authors due to the apparent arbitrariness in the definition of the continuum bins [5]. Furthermore, the generalization of the method to treat the three-body continuum is not obvious.

As an alternative to the binning procedure, other methods have been used to represent the continuum spectrum of a two-body system by a discrete and finite set of square integrable, or  $L^2$ , states such as Laguerre [6,7] or Gaussian [8,9] functions. A family of these states, usually called *pseudostates*, is used to diagonalize the Hamiltonian of the two-body system. The resulting eigenstates are then used within the CDCC calculation in exactly the same way as the continuum bins. In this context, a new basis suitable for continuum discretization has been proposed and applied to the scattering of two-body composite systems in a series of recent works [10–15]. The method generates a discrete representation of the continuum

spectrum starting from the ground state wave function, which is the only needed input. A local scale point transformation (LST) [16,17] that transforms this function into the harmonic oscillator ground state wave function is defined. Once the LST is obtained, the inverse transformation produces from the harmonic oscillator states the wave functions that represent the continuum (and other bound states if they exist) of the two-body system. The corresponding pseudostate set is known as the transformed harmonic oscillator (THO) basis. The method was first developed in Ref. [10] for simple one dimensional problems and later extended in order to check its applicability and limitations [11–15]. In particular, in Ref. [15] it was shown that the combination of the THO discretization method with the coupled channels technique, named CDCC–THO, can be useful to describe continuum effects in nuclear collisions. In Ref. [15], several restrictions were imposed for the sake of simplicity: the deuteron was taken to be a pure  $s$ -state, the effect of Coulomb breakup was neglected, and the nuclear interaction of the proton and the neutron with the target was accepted to induce the coupling just to  $s$ -wave breakup states. Moreover, the deuteron ground state was represented by an analytical wave function. Within this simplified scenario, it was shown that the method was in excellent agreement with the standard CDCC method.

In this work we apply the CDCC–THO method to the reaction  ${}^8\text{B}+{}^{58}\text{Ni}$  at 25.8 MeV, in which the  ${}^8\text{B}$  projectile is modelled as a weakly bound two-body system, proton+ ${}^7\text{Be}$ . This reaction has been extensively analyzed within the standard CDCC formalism [18,19] as well as within the CDCC method with a Gaussian basis [20]. The motivations of this work are the following. First we would like to show that the method can be equally implemented in the usual situation in which the ground state of the system is not known analytically but is calculated numerically. Second, we aim to show that the method can be generalized in a straightforward way to describe the continuum part of the spectrum for arbitrary partial waves. Since the  ${}^8\text{B}$  ground state corresponds mainly to a  $p$ -wave configuration, the THO method provides a discrete representation for the  $\ell = 1$  continuum. We will show below, however, that it can be easily extended to generate also a representation for the  $\ell = 0$  continuum. Finally, we will show that, despite the finite extension and exponential asymptotic

behavior of the THO basis, these states are suitable to describe situations dominated by long range interactions, such as the dipole Coulomb couplings arising in collisions of a loosely bound projectile by heavy ions.

For that purpose, we first present in Sec. II a brief review of the basic formulation of the THO method and describe how it can be extended to different continuum configurations. Then, in Sec. III we present calculations, in which the THO wave functions are used for a coupled channels calculation (CDCC–THO), to show the convergence of the method for several magnitudes related to the  ${}^8\text{B}+{}^{58}\text{Ni}$  reaction at 25.8 MeV. We use the standard CDCC calculations as a reference to compare with. Finally, in Sec. IV we summarize the main results of this work.

## II. THE THO METHOD

The standpoint of the THO method is the ground state wave function of the two-body system, here denoted as  $\phi_{b,\ell_0}(r)$ . The subscript  $\ell_0$  represents the intercluster relative angular momentum. To simplify the notation, we do not consider the intrinsic spins of the fragments. By use of a local scale transformation (LST) [16,17], this wave function is converted into a harmonic oscillator (HO) wave function. Thus, the function  $s(r)$  defining the LST is given by

$$\phi_{b,\ell_0}(r) = \sqrt{\frac{ds}{dr}} \phi_{0,\ell_0}^{\text{HO}}(s(r)). \quad (1)$$

Where  $\phi_{0,\ell_0}^{\text{HO}}(s)$  is the radial part of the HO wave function for the orbital angular momentum  $\ell_0$ . Once the  $s(r)$  function has been obtained, the THO basis is generated by applying the same LST calculated for the ground state to the rest of HO wave functions. Due to the simple analytical structure of the harmonic oscillator wave functions, this is equivalent to multiply the ground state function by the appropriate Laguerre polynomials  $L_n^{\ell+1/2}(s^2)$  [15]

$$\phi_{n,\ell}^{\text{THO}}(r) = [s(r)]^{\ell-\ell_0} L_n^{\ell+1/2}(s(r)^2) \phi_{b,\ell_0}(r). \quad (2)$$

Notice that, by construction, the family of functions  $\phi_{n,\ell}^{\text{THO}}(r)$  are orthogonal and constitute a complete set. Moreover, they decay exponentially at large distances, thus ensuring the correct asymptotic behavior for the bound wave functions. However, in general, these functions are not eigenstates of the internal Hamiltonian. Then, the following step is to diagonalize the Hamiltonian using a truncated THO basis. As a result of the diagonalization a new set of functions, denoted  $\{\phi_{j,\ell}^N(r); j = 0, \dots, N\}$ , with eigenvalues  $\epsilon_0, \dots, \epsilon_N$  are obtained. Here,  $N+1$  is the number of functions retained in the THO basis, ( $j = 0$ ) standing for the ground state. Thus  $\phi_{0,\ell_0}^N(r) = \phi_{0,\ell_0}^{\text{THO}}(r) = \phi_{b,\ell_0}(r)$  and so  $\epsilon_0 = \epsilon_b$ , while the rest of eigenstates constitute our representation of the bound and unbound energy spectrum. Those eigenstates at negative energy will represent bound states of the system. In particular, for  $\ell < \ell_0$ , the diagonalization generates negative energy states, which correspond to occupied states. These states are Pauli forbidden states, that should be excluded from the calculations.

In Ref. [15], the transformation given by Eq. (2) was defined only for continuum states with the same angular momentum  $\ell$  as the ground state. In the present work, we generalize this procedure by applying the same transformation to obtain THO states for  $\ell \neq \ell_0$ . In particular, in the next section we will apply the method to describe the  $\ell = 0$  and  $\ell = 1$  continuum states of the  $p+{}^7\text{Be}$  system.

## III. APPLICATION TO THE ${}^8\text{B}+{}^{58}\text{Ni}$ REACTION

In this section, we apply the THO method to describe the two-body continuum of the proton- ${}^7\text{Be}$  system in the  ${}^8\text{B}+{}^{58}\text{Ni}$  reaction at 25.8 MeV. To simplify the calculations, we neglect the  ${}^7\text{Be}$  and valence proton spins. Therefore, the  ${}^8\text{B}$  ground state is given by a  $\ell = 1, J = 1$  configuration. Using Eq. (2) we generate the THO basis for the  $\ell = 0$  and  $\ell = 1$  states. Then, we retain a finite number of states and diagonalize the  ${}^8\text{B}$  Hamiltonian in this truncated space. The resulting eigenvalues and their associated wave functions constitute a discrete and finite representation of the continuum for the  $p+{}^7\text{Be}$  system.

The bound and continuum states are used to generate the diagonal and nondiagonal coupling potentials that enter the system of coupled equations. In both the standard CDCC and CDCC–THO methods, these coupling potentials are defined as

$$U_{\alpha,\alpha'}(R) = \langle \phi_{n,\ell}^N | U_{[p-\text{Ni}]} + U_{[{}^7\text{Be}-\text{Ni}]} | \phi_{n',\ell'}^N \rangle, \quad (3)$$

with  $\alpha = \{n, \ell\}$ ,  $\alpha' = \{n', \ell'\}$ . The internal wave functions  $\phi_{n,\ell}^N(r)$  are represented by either continuum bins or the THO basis, depending on the discretization method. The proton- ${}^7\text{Be}$  nuclear interaction was represented by a simple Woods-Saxon form with the potential parameters of Esbensen and Bertsch [21]. This interaction is used to generate the ground state wave function for the  ${}^8\text{B}$  system as well as for the diagonalization of the  ${}^8\text{B}$  Hamiltonian in the THO basis. The proton- ${}^{58}\text{Ni}$  interaction was taken from the parametrization of Becchetti and Greenlees [22]. For the  ${}^7\text{Be}-{}^{58}\text{Ni}$  system, we used the interaction of Moroz *et al.* [23] following the choice of other authors [19,20]. All possible couplings ( $s-s$ ,  $s-p$  and  $p-p$ ) were included in the calculations for multipolarities  $\lambda = 0, 1$  and  $2$ . In the standard CDCC calculation, the continuum spectrum was discretized into energy bins of equal momentum width and up to a maximum excitation energy of  $\epsilon_{\text{max}} = 10$  MeV. In particular, we used  $N = 16$  bins for  $\ell = 1$  and  $N = 32$  for  $\ell = 0$ . The bin wave functions were calculated up to 100 fm. For a meaningful comparison, we take the same potential parameters as in the CDCC–THO calculation. The coupled equations were solved for projectile-target orbital angular momenta up to  $L_{\text{max}} = 500$  and integrated up to a radius  $R_{\text{max}} = 500$  fm.

In Fig. 1 we represent the eigenvalues obtained upon diagonalization of the  ${}^8\text{B}$  Hamiltonian in a THO basis with  $N = 20$  states. The vertical axis corresponds to the linear momentum  $k_i = \sqrt{2\mu\epsilon_i}/\hbar$ , where  $\mu$  is the proton- ${}^7\text{Be}$  reduced mass. It should be noticed that these eigenvalues tend to concentrate close to zero energy. As the excitation energy increases, the energy distribution becomes more sparse. It is interesting to note that a deeply bound state

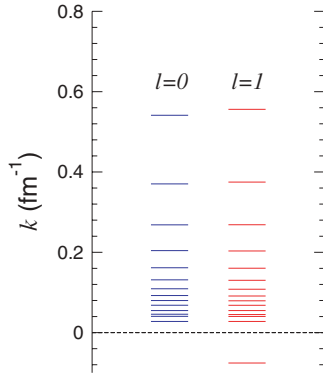


FIG. 1. (Color online) Eigenvalues obtained upon diagonalization of the internal Hamiltonian in a THO basis with  $N = 20$  states for  $s$  and  $p$ -waves. The vertical axis corresponds to the proton- ${}^7\text{Be}$  linear momentum. The  $p$ -state at negative energy corresponds to the ground state.

( $\epsilon \approx -15$  MeV) appears for  $\ell = 0$  (not shown in Fig. 1). This state corresponds to the  $1s$  level of the  ${}^8\text{B}$  nucleus. Since this state is occupied it is removed from our model space. We note also that some eigenvalues may lie at very high energies. In principle, one could include these states in the system of the coupled equations. In practice, however, states at very high energies are very weakly coupled to the ground state and, hence, do not influence the dynamics of the reaction. Besides, the inclusion of these states makes the calculation computationally more intensive and may even lead to convergence problems. For these reasons, in our calculations those states above a certain excitation energy are completely removed from the coupled equations. This maximum energy will depend, indeed, on the particular reaction. In this case, we found that states above 10 MeV have no effect whatsoever on the reaction observables we are studying and, therefore, only those states with excitation energies below this value are retained in our calculations. Notice that states above 10 MeV have been also omitted from Fig. 1.

In Fig. 2 we plot the modulus of some components of the breakup  $S$  matrix for a total angular momentum  $J = 150$  which, assuming a classical trajectory, corresponds to a scattering angle of  $10^\circ$ . As noted in Ref. [20] at these angles breakup is mostly due to the Coulomb interaction. In the standard CDCC, the breakup  $S$  matrix is obtained by dividing the discrete  $S$  matrix to the continuum bins by the square root of the bin width,  $\Delta k_i$ . In the CDCC-THO method, one could apply a similar procedure by assigning a width to each pseudostate. In Ref. [15] we used this approach to calculate the differential breakup cross section from the cross section to individual pseudostates. In particular, we assumed that the width of the  $i$ th pseudostate is approximately given by  $\Delta_i = (\epsilon_{i+1} - \epsilon_{i-1})/2$ . In this work, we adopt a more sophisticated approach, previously proposed in Ref. [24] in the context of the Gaussian expansion pseudostate method. In this method, the breakup  $S$  matrix elements  $S_{\alpha':\alpha}(k)$ , which depend on the continuous variable  $k$ , as well as on the initial and final angular momenta, are obtained by an appropriate superposition of the discrete  $S$  matrix elements  $\hat{S}_{\alpha':\alpha}(k_i)$  resulting from the

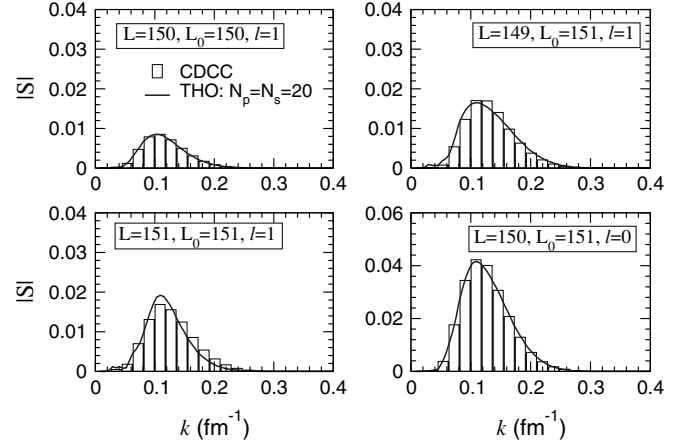


FIG. 2. Breakup  $S$  matrix elements for the total angular momentum  $J = 150$  as a function of the asymptotic  $p+{}^7\text{Be}$  relative momentum.

solution of the coupled-channels equations, as [24]

$$S_{\alpha':\alpha}(k) \approx \sum_{j=1}^N \langle \phi_{k,\ell}^{(s)} | \phi_{j,\ell}^N \rangle \hat{S}_{\alpha':\alpha}(k_j), \quad (4)$$

where  $\phi_{k,\ell}^{(s)}(r)$  is the true scattering wave function for the partial wave  $\ell$  and energy  $\epsilon = \hbar^2 k^2 / 2\mu$ . The sum runs over the set pseudostates included in the coupled-channels calculation. The indexes  $\alpha$  and  $\alpha'$  denote the initial and final channels, that is,  $\alpha = \{g.s.; L_0, \ell_0, J\}$  and  $\alpha' = \{i; L, \ell, J\}$ , where  $L_0$  ( $L$ ) is the initial (final) projectile-target orbital angular momentum.

The histograms represented in Fig. 2 correspond to the standard CDCC calculations, and the lines to the CDCC-THO results calculated with a THO basis with  $N_p = N_s = 20$  states. We verified that increasing the number of basis states does not change the calculated  $S$ -matrices, thus indicating the convergence of the THO method with respect to the basis size. Furthermore, the THO calculation with a  $N_p = N_s = 10$  states gives already a result very close to that presented in Fig. 2. The fast convergence of the THO in this case can be attributed to the fact that the Coulomb interaction tends to populate mainly states in the continuum at low excitation energies, where the density of THO states is higher.

In Fig. 3 we represent the elastic (upper panel) and breakup (lower panel) angular distributions. The standard CDCC calculation is represented in both panels by a thick solid line. The thick dashed lines represent the CDCC-THO calculation with  $N = 40$  states which, as can be seen, is almost identical to the standard CDCC calculation. The dotted line in the upper panel corresponds to the elastic calculation omitting the coupling to the continuum. Since both the CDCC and CDCC-THO use the same ground state wave function and interactions, this calculation is identical in both methods. The thin lines in the bottom panel are the calculated breakup angular distributions including only nuclear breakup.

Next, we study the breakup differential energy cross section,  $d\sigma/dE$ . In the standard CDCC method, a natural way to approximate this quantity is to divide the cross section for

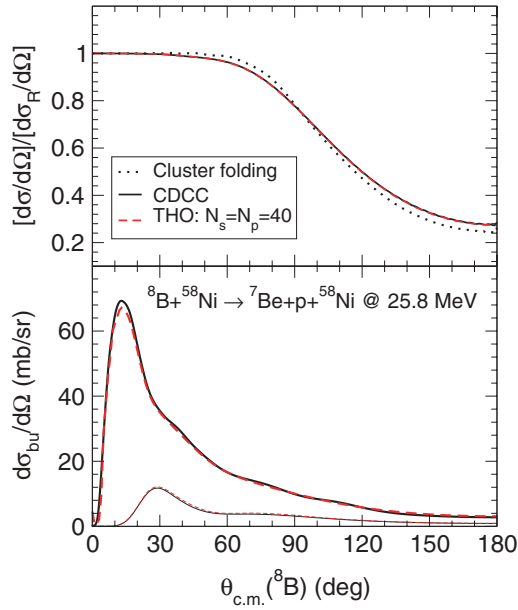


FIG. 3. (Color online) Elastic (upper) and breakup (bottom) angular distribution for the  ${}^8\text{B}+{}^{58}\text{Ni}$  reaction at 25.8 MeV in a model space including  $s$ - and  $p$ -wave states for the  $p+{}^7\text{Be}$  continuum. In both plots, the thick solid line represents the converged CDCC calculation while the thick dashed line corresponds to the CDCC–THO calculation. The same potential parameters and partial waves are used for both calculations. The dotted line in the upper panel is the pure cluster folding calculation without continuum. The thin lines in the bottom panel are the calculations including only nuclear breakup.

each final state by the bin width [2,19]. In the THO method, we could proceed in a similar way, by defining a width for each pseudostate. Alternatively, one can calculate the breakup cross section from the continuous breakup  $S$ -matrices evaluated by means of Eq. (4). Both methods are compared below.

In Fig. 4, we depict the differential energy cross section to  $\ell = 1$  continuum states obtained within the CDCC–THO method with several basis sizes, as indicated by the labels. The lines were obtained using the continuous  $S$  matrices given by Eq. (4) for different basis dimensions. The circles represent the calculation with  $N_s = N_p = 60$  states in which  $d\sigma/dE$  is approximated by dividing the cross section of the  $i$ th pseudostate by the width  $\Delta_i = (\epsilon_{i+1} - \epsilon_{i-1})/2$ . We see that both procedures to obtain  $d\sigma/dE$  give similar results. From this figure we can also infer that the calculation converges as the number of basis states is increased. We notice that, at low excitation energies, the method converges even with a small basis. From this result we can conclude that the method is very suitable to describe Coulomb breakup reactions. Convergence of the breakup cross section for excitation energies above 1 MeV requires a relatively large THO basis. This slower convergence rate is due to the fact that the density of THO states diminishes as the excitation energy increases, and more states are required to describe the excitation into this region. As the number of basis states increases, the solution of the coupled equations becomes slower. However, we note that the actual number of states included in the coupled equations is reduced

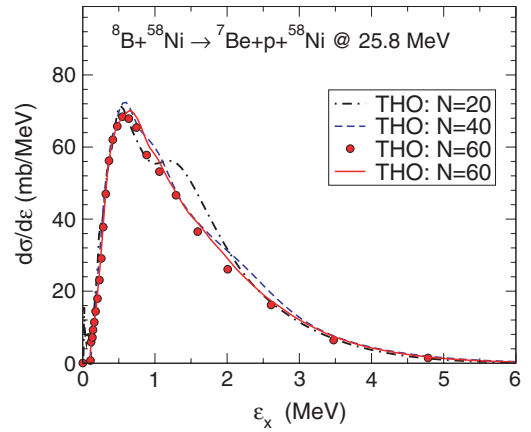


FIG. 4. (Color online) Breakup cross section to  $p$  states as a function of the  ${}^8\text{B}$  internal excitation energy and integrated from  $0^\circ$  to  $180^\circ$ . The lines correspond to the CDCC–THO calculations with different basis dimensions, evaluated from continuous  $S$  matrices according to Eq. (4). The solid circles represent the THO calculation with  $N_s = N_p = 60$  states, in which the cross section to each pseudostate is divided by the estimated energy width (see text).

with respect to the initial basis dimension. As explained above, after the diagonalization only those states with excitation energy below 10 MeV are included in the coupled-channels calculation. In addition, the number of basis states is further reduced by removing those states with excitation energy below  $\sim 0.1$  MeV. Once these two restrictions are applied, the number

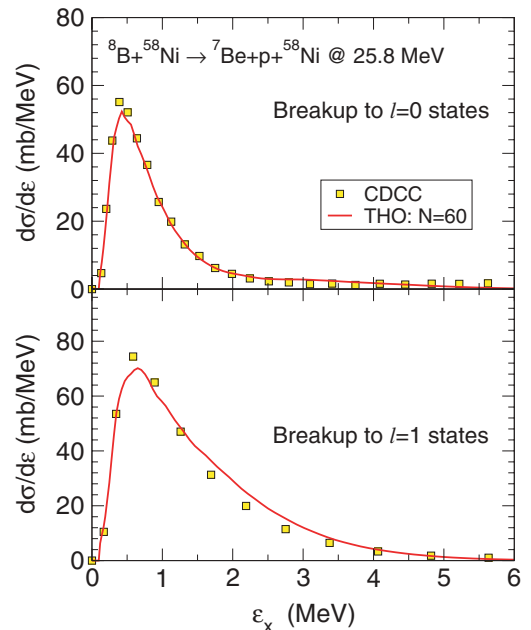


FIG. 5. (Color online) Breakup cross section as a function of the  ${}^8\text{B}$  internal excitation energy for the  ${}^8\text{B}+{}^{58}\text{Ni}$  reaction at 25.8 MeV integrated from  $0^\circ$  to  $180^\circ$ . The squares correspond to the standard CDCC calculations, whereas the solid lines represent the CDCC–THO calculation with a basis with  $N_s = N_p = 60$  states. The separated contribution of  $s$  (upper panel) and  $p$  (lower panel) waves is displayed.

of continuum states actually included in the coupled-channels calculations for the case  $N = 60$  is  $N_{\text{coup}} = 27$  for both the  $s$  and  $p$  waves. We studied also the convergence of the method for the breakup to  $s$ -states. We found that, in this case, convergence is achieved with a smaller number of states, compared to the  $p$ -wave breakup.

Finally, in Fig. 5 we compare the CDCC (squares) and CDCC-THO (solid lines) breakup energy distributions. The latter corresponds to a basis with  $N_s = N_p = 60$  states for which, as we have shown above, good convergence of the THO method is achieved. We present separately the contribution of the  $\ell = 0$  (upper panel) and  $\ell = 1$  (bottom panel) continuum states. We see that both energy distributions are in good agreement with the CDCC calculation.

#### IV. SUMMARY AND CONCLUSIONS

In conclusion, in this work we have presented an extension of the THO method, formerly applied to describe the  $\ell = 0$  deuteron continuum, to generate a discrete representation of the continuum of a two-body system for any partial wave. As in the original formulation, the only *a priori* prerequisite for the application of the method is the knowledge of the ground state wave function of the system, either analytically or numerically. A local scale transformation,  $s(r)$ , is then defined such that it

converts the ground state wave function of the system into the harmonic oscillator ground state. Then, the THO basis is obtained by multiplying the ground state wave function by a set of Laguerre polynomials expressed in the variable  $s(r)$ . This THO basis constitutes a discrete and finite representation of the continuum part of the spectrum with the same intercluster angular momentum as the ground state. For other partial waves, the method is generalized in a straightforward way by simply applying the same scaling transformation. The method has been applied to the reaction  ${}^8\text{B} + {}^{58}\text{Ni}$  at subcoulomb energies, showing a fast convergence with the respect to the number of basis states. Our results agree very well with those obtained with the standard CDCC method. In a recent work, we have successfully extended the method to describe the continuum of a three-body system [25] and the application of the method to describe the collision of a three-body loosely bound system by a target is underway.

#### ACKNOWLEDGMENTS

This work has been partially supported by the Spanish Ministerio de Educación y Ciencia and by the European regional development fund (FEDER) under project Nos. FIS2005-01105, FPA2005-04460, and FPA2003-05958. A.M.M. acknowledges financial support from the Junta de Andalucía.

- 
- [1] G. H. Rawitscher, *Phys. Rev. C* **9**, 2210 (1974).
  - [2] M. Yahiro, Y. Iseri, H. Kameyama, M. Kamimura, and M. Kawai, *Prog. Theor. Phys. Suppl.* **89**, 32 (1986).
  - [3] M. Kamimura, M. Yahiro, Y. Iseri, Y. Sakuragi, H. Kameyama, and M. Kawai, *Prog. Theor. Phys. Suppl.* **89**, 1 (1986).
  - [4] N. Austern, Y. Iseri, M. Kamimura, M. Kawai, G. Rawitscher, and M. Yahiro, *Phys. Rep.* **154**, 125 (1987).
  - [5] T. Sawada and K. Thushima, *Prog. Theor. Phys.* **76**, 440 (1986).
  - [6] J. Röder, H. Ehrhardt, C. Pan, A. F. Starace, I. Bray, and D. V. Fursa, *Phys. Rev. Lett.* **79**, 1666 (1997).
  - [7] I. Bray, *Comput. Phys. Commun.* **114**, 356 (1998).
  - [8] A. Macías, F. Martín, A. Riera, and M. Yáñez, *Phys. Rev. A* **36**, 4179 (1987).
  - [9] E. Hiyama, Y. Kino, and M. Kamimura, *Prog. Part. Nucl. Phys.* **51**, 223 (2003).
  - [10] F. Pérez-Bernal, I. Martel, J. M. Arias, and J. Gómez-Camacho, *Phys. Rev. A* **63**, 052111 (2001).
  - [11] F. Pérez-Bernal, I. Martel, J. M. Arias, and J. Gómez-Camacho, *Few-Body Syst. Suppl.* **13**, 217 (2001).
  - [12] I. Martel, F. Pérez-Bernal, M. Rodríguez-Gallardo, J. M. Arias, and J. Gómez-Camacho, *Phys. Rev. A* **65**, 052708 (2002).
  - [13] F. Pérez-Bernal, I. Martel, J. M. Arias, and J. Gómez-Camacho, *Phys. Rev. A* **67**, 052108 (2003).
  - [14] M. Rodríguez-Gallardo, J. M. Arias, and J. Gómez-Camacho, *Phys. Rev. C* **69**, 034308 (2004).
  - [15] A. M. Moro, J. M. Arias, J. Gómez-Camacho, I. Martel, F. Pérez-Bernal, R. Crespo, and F. Nunes, *Phys. Rev. C* **65**, 011602(R) (2002).
  - [16] M. V. Stoitsov and I. Z. Petkov, *Ann. Phys. (NY)* **184**, 121 (1988).
  - [17] I. Z. Petkov and M. V. Stoitsov, *Nuclear Density Functional Theory, Oxford Studies in Physics* (Clarendon, Oxford, 1991).
  - [18] F. M. Nunes and I. J. Thompson, *Phys. Rev. C* **59**, 2652 (1999).
  - [19] J. A. Tostevin, F. M. Nunes, and I. J. Thompson, *Phys. Rev. C* **63**, 024617 (2001).
  - [20] T. Egami, K. Ogata, T. Matsumoto, Y. Iseri, M. Kamimura, and M. Yahiro, *Phys. Rev. C* **70**, 047604 (2004).
  - [21] H. Esbensen and G. F. Bertsch, *Nucl. Phys.* **A600**, 37 (1996).
  - [22] F. D. Becchetti and G. W. Greenlees, *Phys. Rev.* **182**, 1190 (1969).
  - [23] Z. Moroz *et al.*, *Nucl. Phys.* **A381**, 294 (1982).
  - [24] T. Matsumoto, T. Kamizato, K. Ogata, Y. Iseri, E. Hiyama, M. Kamimura, and M. Yahiro, *Phys. Rev. C* **68**, 064607 (2003).
  - [25] M. Rodríguez-Gallardo, J. M. Arias, J. Gómez-Camacho, A. M. Moro, I. J. Thompson, and J. A. Tostevin, *Phys. Rev. C* **72**, 024007 (2005).